

# All-cellulose composites from unbleached hardwood kraft pulp reinforced with nanofibrillated cellulose

M. Alcalá · I. González · S. Boufi · F. Vilaseca · P. Mutjé

Received: 27 August 2013 / Accepted: 11 October 2013 / Published online: 6 November 2013  
© Springer Science+Business Media Dordrecht 2013

**Abstract** In the present work, nanofibrillated cellulose (NFC) from bleached eucalyptus pulp was prepared, characterized and used as reinforcement in an unbleached eucalyptus fiber matrix. First, the NFC was fabricated through TEMPO-mediated oxidation and characterized for the degree of polymerization, water retention value, cationic demand and carboxyl content. Intrinsic mechanical properties were also calculated by applying the rule of mixtures, which determines the coupling ( $f_c$ ) and efficiency factor ( $\eta_e$ ) of cellulose nanofibrils within the matrix. The results showed that the average intrinsic tensile strength and Young's modulus of NFC are estimated to be 6,919 MPa and 161 GPa, respectively. After characterization, the NFC was used as reinforcement in the preparation of biocomposites in the form of paper handsheets, which were physically and mechanically

analyzed. The presence of NFC induced an increase in the density of biocomposites and significant enhancement of the mechanical properties as well as an important reduction in porosity. Finally,  $f_c$  and  $\eta_e$  were determined from the mean intrinsic properties.

**Keywords** Nanofibrillated cellulose · Unbleached kraft pulp · Mechanical properties · Intrinsic mechanical properties · Biocomposites

## Introduction

Paper and cardboard can be considered as biocomposites (Sehaqui et al. 2011) formed by a porous lignocellulosic fibrous network where fiber–fiber bonds occur by mechanical cross linking and physical–chemical interactions, such as van der Waals forces and hydrogen bonding (Marais and Wågberg 2012). Traditionally, physical and mechanical properties of paper have been improved by means of mechanical beating (Molin and Daniel 2004; Mutjé et al. 2006) and also currently by enzymatic treatment (Pèlach et al. 2003; González et al. 2013). Beating causes an increase in the specific surface area by fibrillation of the fiber's outer layers and swelling, leading to an enhancement of their linking capability (Mutjé et al. 2005). Tensile strength and other mechanical properties in paper depend on the intrinsic

---

M. Alcalá  
PRODIS Group, Department of Organization, Business Management and Product Design, University of Girona, EPS Campus Montilivi, 17071 Gerona, Spain

I. González (✉) · F. Vilaseca · P. Mutjé  
Group LEPAMAP, Department of Chemical Engineering, University of Girona, c/M. Aurèlia Campmany, No. 61, 17071 Gerona, Spain  
e-mail: israel.gonzalez@udg.edu

S. Boufi  
Laboratoire des Sciences des Matériaux et Environnement, Faculté des Sciences de Sfax, Université de Sfax, Sfax, Tunisia

strength of fibers, the magnitude of binding forces between fibers and the amount of binds per volume. However, mechanical beating also implies damage of fibers and increasing of the fines fraction. This represents a problem for the subsequent exploitation of recycled paper because subsequent beatings will shorten and degrade the fibers, thus diminishing their original properties. The use of nanofibrillated cellulose (NFC) contributes significantly to increasing the lignocellulosic fibrous network's specific surface area (SSA) as a consequence of NFC's nanometric size. Slurry of unbeaten lignocellulosic fibers presents an SSA of approximately  $1 \text{ m}^2/\text{g}$ , whereas NFC from bleached hardwood pulp exhibits SSA values superior to  $30 \text{ m}^2/\text{g}$  (Spence et al. 2011). This situation leads to a mixture where two phases are found: one at the microscale and another at the nanoscale. For example, the application of 6 wt% of NFC to a lignocellulosic fibrous slurry generates a phase with an SSA of  $100 \text{ m}^2$  (100 g of lignocellulosic fibers) and another one of  $330 \text{ m}^2$  ( $55 \text{ m}^2/\text{g}$ ) made of NFC. This larger SSA also affects the cationic demand of the slurry biocomposite (Vilaseca et al. 2004), which is significantly inferior in lignocellulosic fibers compared to NFCs (Klemm et al. 2011).

Regarding the intrinsic properties of NFC, many efforts have been made during the last years to estimate both tensile strength and Young's modulus of a single NFC fiber. The results reported have been somehow diverse. Yano and Nakahara (Yano and Nakahara 2004) reported a value of at least 2 GPa based on experimental results for the tensile strength of 1.7 GPa from kraft pulp when 70–80 % of microfibrils were distributed parallel to the fiber direction. The same authors reported a Young's modulus of up to 134 GPa. Zimmerman et al. (2004) reported that the tensile strength of the crystal structure in a microfibril varies from approximately 0.8 to 10 GPa, whereas Young's modulus would be as high as 250 GPa. Iwamoto et al. (2009) performed measurements of Young's modulus of a single NFC strand through atomic force microscopy (AFM) by the three-point bending test. Their experiments on NFC obtained by TEMPO-mediated oxidation delivered a Young's modulus of 145 GPa. More recently, Saito et al. (2013) reported tensile strength values of 1.6–3 GPa for NFC from wood, with an estimated Young's modulus of 30–40 GPa for wood fiber. The variety in results, mainly in Young's modulus estimations, may

be a consequence of the different techniques used during the fabrication of NFC, the cellulose source and the methodology applied for determining the intrinsic properties of fibers.

What is clear is that the incorporation of NFC into lignocellulosic fibrous slurries should result in an increase of the physical–mechanical properties of the biocomposites produced from the mixture. The presence of NFC generates a propitious interface (Marais and Wågberg 2012), without the need for any prior beating. In the present work, we fabricated and characterized NFC obtained from bleached eucalyptus pulp through TEMPO-mediated oxidation at pH 7. Then, the physical and intrinsic mechanical properties of the ensuing NFC were studied. Finally, the NFC was used as reinforcement in unbleached eucalyptus pulp-based biocomposites, which were later characterized from their mechanical and thermal properties.

## Materials and methods

### Materials

For the preparation of NFC, commercial dried bleached eucalyptus pulp from La Montañanesa (Grupo Torraspapel, Zaragoza, Spain) was used as starting material. Polyvinyl alcohol (PVA) (Mw 30000–70000, 87–90 % hydrolyzed) was used as a matrix for composites with the aim to study NFC's intrinsic properties. For the preparation of biocomposites, once-dried unbleached eucalyptus pulp was used as received. Silica colloidal and cationic starch, used as retention agents in the fabrication of biocomposites, were kindly given by Torraspapel S.A. (Sarrià de Ter, Girona, Spain). For the oxidation process prior to defibrillation, 2,2,6,6-tetramethylpiperidine-1-oxyl radical (TEMPO), sodium bromide (NaBr), sodium chlorite ( $\text{NaClO}_2$ ) and sodium hypochlorite solution ( $\text{NaClO}$ ) were acquired from Sigma-Aldrich and used as received.

### Methods

#### *Preparation of NFC*

The TEMPO-mediated oxidation of cellulose fibers was performed at neutral pH conditions according to the methodology reported by Besbes et al. (2011). The

fibrillation process was performed by passing a 1–2 wt% fiber-water suspension through a high-pressure homogenizer (NS1001L PANDA 2 K-GEA). The equipment was operated from 300 to 600 bar pressure and 60–70 °C. The process was repeated several times until a transparent, gel-like product was obtained.

#### Characterization of NFC

The degree of polymerization (DP) was determined from intrinsic viscosity measurements using cupriethylenediamine as solvent at 25 °C, according to UNE 57-039-92. The measurements were carried out on dried NFC samples. The viscosimetric average molecular weight was calculated from the following equation:  $\eta = K \cdot M^a$ , where  $\eta$  is the intrinsic viscosity,  $K$  is an empirical relationship for the cellulose-cupriethylenediamine solvent system, and  $a$  has been estimated as 2.28 (Henriksson et al. 2008).  $M$  is the viscosity average molecular weight, and  $a$  is a factor determined by the form adopted by the polymer chain, considered as 0.76 (Henriksson et al. 2008). The water retention value (WRV) was measured according to TAPPI UM 256. Samples were centrifuged in a Sigma 6K15 centrifuge. In order to retain the NFC during centrifugation, a nitrocellulose membrane with a 0.65- $\mu\text{m}$ -diameter pore was used at the bottom of the centrifuge bottles. Once centrifuged, only the NFC in contact with the membrane was removed, weighed and then dried at  $105 \pm 2$  °C for 24 h in containers of previously measured weight. The average water retention value was then calculated according to Eq. 1:

$$\text{WRV} = \frac{W_w - W_d}{W_d} \quad (1)$$

where  $W_w$  is the wet weight (g) and  $W_d$  the dry weight (g). The carboxyl content of oxidized cellulose was calculated by conductometric titration according to the methodology published by Da Silva et al. (2003). The carboxyl content (CC) is given by Eq. 2:

$$\text{CC} = 162(V_2 - V_1)c[(w - 36(V_2 - V_1))c]^{-1} \quad (2)$$

where  $V_1$  and  $V_2$  are the equivalent volumes of added NaOH solution (L),  $c$  is the NaOH concentration (mol/L), and  $w$  the weight of the oven-dried sample (g). The results indicate the average mmols of the

–COOH groups per gram of NFC. The cationic demand of NFC fibers was determined with a Mütek PCD 04 particle charge detector. First, 0.04 g. of NFC (dried weight) was diluted in 1 L distilled water and dispersed with a pulp disintegrator for 10 min at 3,000 rpm. Next, 10 mL was taken and mixed with 25 mL of cationic polymer polydiallyldimethylammonium chloride (polyDADMAC) for 5 min with magnetic stirring. After this time, the mixture was centrifuged in a Sigma 6K15 centrifuge for 90 min at 4000 RPM (1969 RCF). Then, 10 mL of the supernatant was taken to the Mütek equipment. Anionic polymer (Pes-Na) was then added to the sample drop by drop with a pipette until the equipment reached 0 mV. The volume of anionic polymer consumed was used to calculate the cationic demand though Eq. 3:

$$\text{CD} = - \frac{(C_{\text{PolyD}} \cdot V_{\text{PolyD}}) - (V_{\text{Pes-Na}} \cdot C_{\text{Pes-Na}})}{W_{\text{sample}}} \quad (3)$$

where CD is the cationic demand ( $\mu\text{eq/L}$ ),  $C_{\text{PolyD}}$  = cationic polymer concentration (g/L),  $V_{\text{PolyD}}$  = used volume of cationic polymer (mL),  $C_{\text{Pes-Na}}$  = anionic polymer concentration (g/L),  $V_{\text{Pes-Na}}$  = used volume of anionic polymer (mL) and  $W_{\text{sample}}$  = sample's dry weight (g).

#### Intrinsic properties of NFC via PVA–NFC composites

Polyvinyl alcohol and nanofibrillated cellulose gel were mixed in a Brabender blender at 80 rpm and 210 °C for 20 min. The resulting composite was then molded-injected using the single-screwed Meteor 40 (Mateu & Sole) equipment operating at 220 °C. The first and second injection pressures were set at 125 and 50 kg/cm<sup>2</sup>, respectively. The tensile-test samples thus fabricated were 115 mm long, 13 mm wide and 3 mm thick.

#### Determination of $\sigma_t^{NP}$ and $E_t^{NP}$ from nanopaper

Nanofibrillated cellulose handsheets (nanopaper) were fabricated in order to experimentally determine the mechanical properties of nanofibrils. An amount of NFC gel equivalent to 2.14 g of dried pulp was suspended in 2 L of distilled water and dispersed in the pulp disintegrator. The NFC was then dewatered in Rapid-Köthen-type sheet former equipment. The screen in the stock container was provided with a

0.65- $\mu\text{m}$  nitrocellulose filter membrane to retain the NFC. The obtained nanopaper was then put between two absorbing sheets and vacuum dried for 15–20 min. Finally, the handsheets were conditioned in a weather chamber at 25 °C and 50 % humidity for 24 h before mechanical testing.

#### *Fabrication of biocomposites*

Dried unbleached eucalyptus pulp was disintegrated in water at 180000 revolutions in a pulp disintegrator. NFC was added to the slurry at the beginning of the process. The amount of NFC was calculated to obtain 0, 3, 6, 9 and 12 wt% NFC-reinforced biocomposites. The resulting slurry was subsequently dispersed in water and stirred. Silica colloidal and cationic starches were added during stirring in amounts of 0.8 and 0.5 wt%, respectively, with continued stirring for 30 min at 500 rpm. The biocomposites were fabricated in the form of paper sheets in a Rapid-Köthen sheet former (ISP model 786 FH) according to ISO 5269-2 and conditioned in a weather chamber at 25 °C and 50 % humidity for 24 h before mechanical testing.

#### *Mechanical and physical characterization*

Tensile experiments for PVA-based composites were carried out in an IDM universal testing machine equipped with a 5-kN load cell. Testing was performed according to ISO standards 1924-1 and 1924-2. The gap between clamping jaws was set to 115 mm, and the cross head speed was set to 2 mm/min. Preload was set at 1 N. Results are the average of at least five samples. Biocomposites and nanopaper sheets were tested in an Instron universal testing machine provided with a 2.5-kN load cell. The distance between clamps was set at 150 mm. Preload was 0.1 N and cross-head speed 15 mm per minute. The testing specimens were cut down to stripes of 20 mm length and 15 mm width. The results are the average of at least five samples. Density was calculated from the basis weight, thickness and dimensions of the handsheets. Porosity was determined from the density of the biocomposite by applying the next Eq. (4):

$$\text{Porosity}(\%) = 100 \cdot \left( 1 - \frac{\rho_{\text{sample}}}{\rho_{\text{cellulose}}} \right) \quad (4)$$

where the  $\rho_{\text{sample}}$  is the density of the biocomposites, and  $\rho_{\text{cellulose}}$  is the density of cellulose, assumed to

be 1.6 g/cm<sup>3</sup> (Henriksson et al. 2011; Saito et al. 2013).

#### *Thermal characterization*

Dynamic mechanical analyses were performed in a DMTA Mettler Toledo analyzer, model DMA/SDTA861. Samples were cut down to pieces of 5.5 mm length and 5 mm width. The analysis temperature started at –50 °C and finished at 250 °C, with a heating rate of 3 °C per minute. The frequency was set at 10 Hz.

#### *Electronic microscopy*

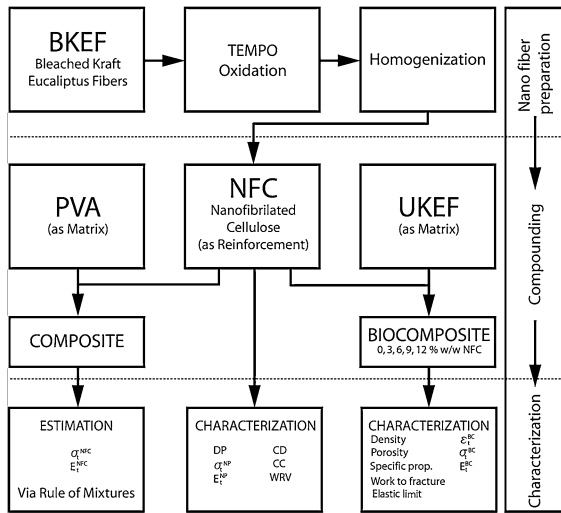
The external appearance of nanopaper and all-cellulose composites was observed through TEM and SEM observation. Dried samples for SEM observation had been previously prepared by gold sputtering; the observation was performed in a Zeiss DSM 960. TEM samples were treated with uranyl acetate for negative staining. The TEM observation was done in a Zeiss EM 910.

Figure 1 presents a summary of the different stages in the fabrication and characterization of the NFC and its composites.

## **Results and discussion**

### **Characterization of NFC**

In Table 1 the results for the characterization of NFC are resumed. The intrinsic viscosity indicated an average degree of polymerization (DP) of 423. This value situates our NFC in the group of nanocelluloses with low DP reported by Henriksson et al. 2008 (from DP 410 to 1100), who reported a correlation between the DP of MFC and the tensile strength of films made thereof. DP is directly related to the intrinsic tensile strength of NFC; therefore, cellulose nanofibrils with higher DP would present better mechanical properties. In the case of our nanopapers, mechanical tests delivered a tensile strength ( $\sigma_t^{\text{NP}}$ ) of 135 MPa (Table 1), a value very similar to that reported by Henriksson et al. (2008) for nanopaper with DP 410. It has been proposed that breaking in NFC nanopaper occurs by slippage of the extended cellulose chains rather than by the covalent bond breakage expected at high DP (Mark 1967; Wainwright et al. 1982).



**Fig. 1** Flow chart of NFC production and characterization; PVA polyvinyl alcohol; UKEF unbleached Kraft eucalyptus pulp;  $\sigma_t^{NFC}$  intrinsic tensile strength of NFC;  $E_t^{NFC}$  intrinsic Young’s modulus of NFC; DP degree of polymerization; CD cationic demand;  $\sigma_t^{NP}$  tensile strength of nanopaper;  $E_t^{NP}$  Young’s modulus of nanopaper; CC carboxyl content of NFC; WRV water retention value;  $\sigma_t^{NP}$  and  $E_t^{NP}$  tensile strength and modulus of nanopaper, respectively;  $\sigma_t^{NFC}$  and  $E_t^{NFC}$  intrinsic tensile strength and modulus of NFC

Regarding Young’s modulus ( $E_t^{NP}$ ), its value of 11.5 GPa is lower than that reported by Henriksson et al. (2008), who found values of 13.7 GPa for nanopapers with DP 410. Table 1 also shows the WRV, an empirical parameter that measures the capacity of a test pad of fibers to hold water. It is typically used as a way to indirectly measure the beating degree of papermaking slurries and depends on the internal fibrillation of fibers. NFC presented a WRV average value of 17 g/g. This result is well above those reported for typical beaten papermaking pulps. Dang et al. (2007) pointed out an increase in the WRV of softwood bleached kraft fibers after TEMPO-mediated oxidation, whereas Yano and Nakagaito found that the WRV of NFC suspensions correlated

with both the Young’s modulus and the tensile strength (Klemm et al. 2011). Table 1 also shows the cationic demand of NFC obtained through polyelectrolyte titration, a technique based on the ability of polyelectrolytes to form complexes with other oppositely charged polyelectrolytes (direct titration) or surfaces (indirect titration) (Rouger and Mutjé 1984; Klemm et al. 2011). Cellulosic components become negative in aqueous suspensions because of the ionization of carboxylic groups and the absorption of some ions in aqueous suspensions (Mutjé et al. 2006). The cationic demand for NFC was found to be 859  $\mu\text{eq-g/g}$ . It can be speculated that this parameter might follow a similar behavior as that of fines in papermaking slurries, where fines have a higher cationic demand for neutrality than fibers (Carrasco et al. 1998; Orblin and Fardim 2011). Concerning carboxyl content, our samples presented 0.4 mmol of COOH groups per g of fiber. This parameter is the main factor that determines the extent of the nanofibrillation of the fibers and the degree of NFC polymerization.

As a part of the characterization of NFC, the intrinsic mechanical properties were also determined by fabricating PVA-based nanocomposites reinforced with NFC. The nanocomposites were then mechanically tested, and the ensuing results were analyzed using mathematical models. The term intrinsic mechanical property refers to the intrinsic tensile strength ( $\sigma_t^{NFC}$ ) and Young’s modulus ( $E_t^{NFC}$ ) of NFC. Table 2 shows the mechanical properties of PVA/NFC composite materials. In this table,  $V^{NFC}$  represents the volume fraction of NFC within the composite, calculated from the density of the sample and by assuming the density of NFC to be 1.6  $\text{g/cm}^3$ .  $\sigma_t^C$  and  $E_t^C$  are the tensile strength and Young’s modulus of the composites, respectively.

The results indicate that the addition of NFC to the polymer matrix increases both the tensile strength and Young’s modulus of the composite in comparison to

**Table 1** Results for the characterization of NFC

DP	$\sigma_t^{NP}$ (MPa)	$E_t^{NP}$ (GPa)	WRV (g/g)	CD ( $\mu\text{eq-g/g}$ )	CC (mmol/g)	$\sigma_t^{NFC}$ (MPa)	$E_t^{NFC}$ (GPa)
423	135 $\pm$ 3.2	11.5 $\pm$ 0.67	17	859	0.4	6,919 $\pm$ 679.45	161.05 $\pm$ 6.15

$\sigma_t^{NP}$  and  $E_t^{NP}$  tensile strength and Young’s modulus of nanopaper, respectively;  $\sigma_t^{NFC}$  and  $E_t^{NFC}$  intrinsic tensile strength and Young’s modulus of the NFC

DP degree of polymerization; WRV water retention value; CD cationic demand; CC carboxyl content



the neat matrix. This increase is in relation to the amount of NFC added to PVA, following a linear evolution (Fig. 2).

A good interface is crucial in the transmission of stress and load from the matrix to the reinforcement. Since both NFC and PVA have available OH groups, the formation of hydrogen bonds is expected (Lue et al. 2008). As evidence, the increase in NFC content leads to 48, 60 and 90 % improvement in the composite's tensile strength. The reinforcing effect of NFC has been attributed to the direct interaction between the fiber and the polymer, the intrinsic strength of NFC and the formation of a rigid web-like structure embedded within the matrix (Qua et al. 2009). Zimmerman et al. (2004) noted that, for the formation of a networked structure in PVA composites, a filling threshold should be achieved; in our results, composites with a filling threshold of 2.25 % already presented enhancement of mechanical properties.

The estimation of the intrinsic tensile strength of NFC is possible by resolving  $\sigma_t^{\text{NFC}}$  from the modified rule of mixtures (Eq. 5):

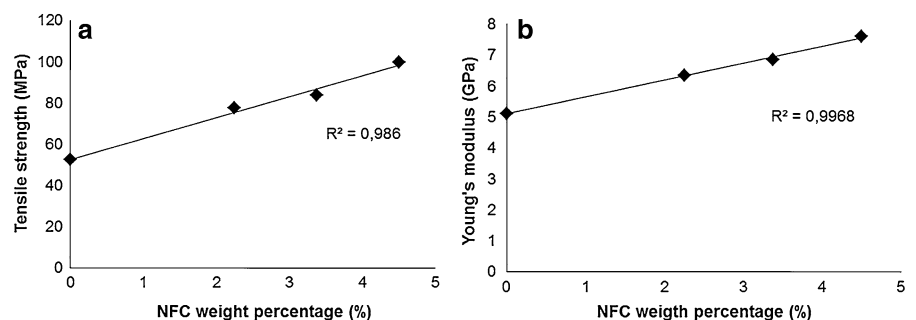
$$\sigma_t^C = f_c \cdot \sigma_t^{\text{NFC}} \cdot V^{\text{NFC}} + (1 - V^{\text{NFC}}) \cdot \sigma_t^{(m^*)} \quad (5)$$

where  $\sigma_t^C$ ,  $\sigma_t^{\text{NFC}}$  and  $\sigma_t^{m^*}$  represent the ultimate tensile strength of the composite, the reinforcing NFC fiber

**Table 2** Mechanical properties for NFC/PVA composites and intrinsic mechanical properties for NFC

NFC (w/w %)	$V^{\text{NFC}}$ (v/v)	$\sigma_t^C$ (MPa)	$E_t^C$ (GPa)	$\sigma_t^{\text{NFC}}$ (Mpa)	$E_t^{\text{NFC}}$ (GPa)
0	0	52.40 ± 5.2	5.10 ± 0.2	–	–
2.250	0.019	77.65 ± 7.6	6.35 ± 0.5	7,552	162.0
3.375	0.0275	83.80 ± 6.3	6.85 ± 0.3	6,201	154.5
4.500	0.0368	99.70 ± 5.7	7.60 ± 0.5	7,004	166.7

**Fig. 2** Evolution of tensile strength (a) and Young's modulus (b) in PVA-based composites as a function of NFC content



and the matrix at the failure of the composite, respectively;  $V^{\text{NFC}}$  is the volume fraction of the reinforcement and  $f_c$  the compatibility factor. This last parameter is related to the degree of adhesion at the interface between the matrix and reinforcement; it represents the reinforcing capacity of the NFC within the composite (Vilaseca et al. 2010). Values for  $f_c$  close to 1 represent the maximum reinforcing capacity of the filler, though typical values for good quality interfaces are between 0.17 and 0.28, with an average 0.208 (Fu and Lauke 1996). For the present study, the compatibility factor is considered to be 0.20 (Sanadi et al. 1994). The tensile strength of PVA at the failure of composite ( $\sigma_t^{m^*}$ ) was interpolated from the stress-strain curve of the PVA matrix. The intrinsic tensile strength calculated for NFC in every composite is also shown in Table 2; the average value of the three results is 6919 MPa, and the highest value (7552 MPa) was calculated from the sample with 2.25 wt% of NFC. The Young's modulus of a single NFC fiber can be calculated using the Hirsch model (Rodríguez et al. 2010; López et al. 2011), which is based on the combination of parallel and series models of the rule of mixtures model (Eq. 6):

$$E_t^C = \beta(E_t^{\text{NFC}} \cdot V^{\text{NFC}} + E_t^m \cdot (1 - V^{\text{NFC}})) + (1 - \beta) \frac{(E_t^{\text{NFC}} \cdot E_t^m)}{(E_t^m V^{\text{NFC}} + E_t^{\text{NFC}}(1 - V^{\text{NFC}}))} \quad (6)$$

Here  $E_t^C$ ,  $E_t^{\text{NFC}}$  and  $E_t^m$  represent the Young's moduli of the composite material, the reinforcing NFC and the matrix, respectively; as in Eq. 1,  $V^{\text{NFC}}$  represents the volume fraction of NFC. The parameter  $\beta$  determines the stress transfer between the fiber and the matrix. It depends on the fiber orientation, fiber length and stress amplification effect at the fiber ends (Marais and Wågberg 2012). According to several authors (Kalaprasad et al. 1997; Rodríguez et al. 2010;

López et al. 2011), the theoretical and experimental values can fit when  $\beta$  is 0.4, whereas Vilaseca et al. 2010 report experimental values of 0.4335. In the present study, we considered the value of  $\beta$  to be 0.4. The results obtained showed a Young's modulus average value of 161.05 GPa, a value slightly superior to those found in the literature (Yano and Nakahara 2004; Zimmermann et al. 2004; Iwamoto et al. 2009; Saito et al. 2013). If this value is applied to the rule of mixtures equation modified for calculation of Young's modulus (Eq. 7), it is possible to calculate the efficiency factor ( $\eta_e$ ), which is related to the length and orientation of a fiber within a composite:

$$E_t^C = \eta_e \cdot E_t^{\text{NFC}} \cdot V^{\text{NFC}} + E_t^m \cdot V^m \quad (7)$$

Here  $E_t^C$ ,  $E_t^{\text{NFC}}$  and  $E_t^m$  represent, as in Eq. 2, the Young's moduli of the biocomposite, NFC and the matrix, respectively. In the case of the Young's modulus of the composite, an efficiency factor  $\eta_e$  of 0.440 and 0.438 was calculated for the composites with 2.25 and 4.50 wt% volume fractions, respectively. Other authors (Gironès et al. 2007; Vilaseca et al. 2010) reported efficiency factor values ranging from 0.34 to 0.51. It is important to highlight the significance of the coupling and efficiency factor in Eqs. 1 and 2. The rule of mixtures assumes a perfect adhesion between the matrix and reinforcement, but this is not totally achieved in practice (Chakraborty et al. 2006). For this reason, the introduction in the rule of mixtures of a variable that accounts for the quality in the interface between the matrix and reinforcement becomes necessary. The theoretical values for Young's modulus presented up to now are in accordance with what has

been reported by other authors. However, the tensile strength is somehow lower; it is generally accepted that the theoretical tensile strength value of a solid material is approximately a tenth of its Young's modulus (Young and Lovell 1981). However, this should only be considered in the case of materials without mechanical defects. Processing of cellulose nanofibrils, as well as chemical modification, possibly introduces damage of the fiber structure, producing cracks and delamination on the surface, which function as starters of failure when the material is subjected to stress. Therefore, the intrinsic strength of single cellulose nanofibrils should be higher.

SEM and TEM microphotography indicated that NFC diameters are within the nanometer range (Fig. 5). TEM (Fig. 3, picture A) allowed the observation of NFC, which presented diameters of 10–20 nm.

SEM images were taken from nanopaper samples in order to observe how the NFC is arranged within the structure. Picture b shows that most of the nanofibrils are randomly distributed, with the presence of larger fibers in the range of up to 100 nm. The observations confirm that NFC widths are below the  $\mu\text{m}$  range. The length of NFC could not be determined because of the heavy entanglement of nanofibrils and the difficulty to differentiate their ends.

#### Characterization of biocomposites from unbleached eucalyptus fibers/NFC

In Table 3, the physical and mechanical properties of the biocomposites fabricated from unbleached

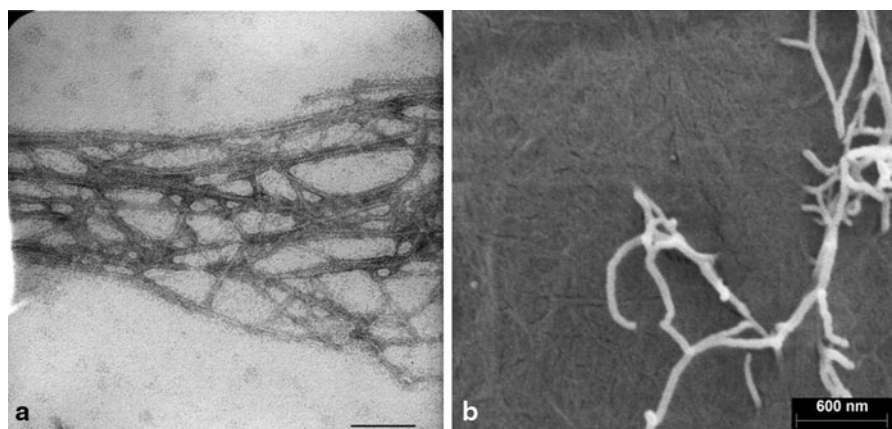


**Fig. 3** TEM (a) and SEM (b) microphotographies of NFC samples. The black bar in a indicates 75 nm

eucalyptus fiber reinforced with different amounts of NFC are summarized. The density, calculated from the basis weight, thickness and dimensions of the samples, increased gradually with the addition of NFC, which means that the composite became more compact. Samples with 9 wt% of NFC presented the highest increase of density (24 %) compared to the neat matrix. Probably, a major availability of specific surface area is the main reason behind this increase. However, further addition of NFC did not add any significant improvement. A linear evolution of this parameter can be observed until samples with 9 wt% of NFC. Perhaps, higher amounts of NFC require more dispersion (energy) applied to the eucalyptus fiber/NFC slurry in order to achieve a good distribution of the nanofibrils between the larger fibers, which would translate into denser biocomposites due to better interaction between nano- and macrofibrils. In fact, the same reasoning can be applied to the behavior seen in Young's modulus, where samples with 12 wt% of NFC did not show significant improvement compared to biocomposites with 9 wt% of NFC. The presence of NFC also produced a reduction in biocomposites' porosity until 9 wt% of NFC content. This behavior was expected since density already showed the formation of a more compact and solid fiber network.

Even though biocomposites with 12 wt% of NFC presented possible dispersion difficulties, they showed the more significant strength improvement by increasing 169 % with respect to the non-reinforced counterpart. Young's modulus also showed an enhancement, and the best value was found in biocomposites with 9 wt% of NFC. Interestingly, the evolution in Young's modulus strongly disagreed with what is reported by Sehaqui et al. (2011), whose results did not increase with the addition of growing amounts of NFC. Strain at break increased up to 59 % in biocomposites with 9 wt% of NFC, though samples with 12 wt% did not present further enhancement. Specific tensile strength and modulus behaved similarly, increasing almost linearly as more NFC was added to the biocomposite, except in samples with 12 wt% of NFC. Work to fracture showed important increases of 570, 800, 1157 and 1163 % for composites reinforced with 3, 6, 9 and 12 wt%, respectively. Stress-strain curves in tension from all the composites are presented in Fig. 4. The curves show a linear elastic region at early deformations, without any structural damage. Next, a yielding knee follows that probably corresponds to debonding

**Table 3** Mechanical properties of biocomposites reinforced with different percentages of NFC

NFC (wt%)	Density (gr/cm <sup>3</sup> )	Porosity (%)	$\sigma_t^{bc}$ (MPa)	$E_t^{bc}$ (GPa)	$\epsilon_t^{bc}$ (%)	$\sigma_t^{bc}$ (*) (MPa)	Specific $\sigma$ (MPa cm <sup>3</sup> /g)	Specific E (GPa cm <sup>3</sup> /g)	Work to fracture (MJ/m <sup>3</sup> )
0	0.547 ± 0.01	63.55 ± 0.2	19.75 ± 2.07	3.85 ± 0.45	1.20 ± 0.2	5.22 ± 1.14	36.1	6.4	0.061 ± 0.030
3	0.594 ± 0.02	60.42 ± 0.3	32.75 ± 3.26	4.41 ± 0.19	1.90 ± 0.1	9.81 ± 2.11	55.15	7.4	0.409 ± 0.074
6	0.621 ± 0.02	58.57 ± 0.2	41.30 ± 2.81	5.30 ± 0.28	1.92 ± 0.1	12.57 ± 2.08	66.50	8.55	0.549 ± 0.072
9	0.678 ± 0.01	54.81 ± 0.1	50.05 ± 6.80	6.12 ± 0.45	2.06 ± 0.3	14.11 ± 1.12	73.80	9.02	0.767 ± 0.212
12	0.671 ± 0.02	55.25 ± 0.1	53.20 ± 5.40	5.95 ± 0.33	2.00 ± 0.2	18.70 ± 1.21	79.28	8.86	0.771 ± 0.120

(\*At yield)



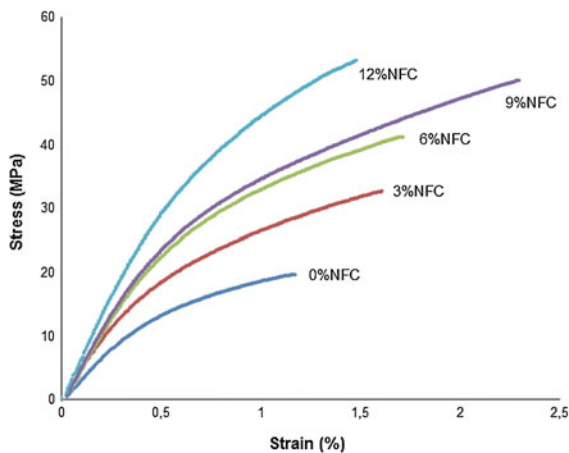


**Fig. 4** Stress-strain curves in the tension of the unbleached eucalyptus pulp/NFC composites. Content of NFC in percentage is represented next to the curve

of eucalyptus fibers (Sehaqui et al. 2011). This knee appears later as NFC is added to the biocomposite because of the improvement in fiber-fiber bonds. The increase in the limit of elasticity confirms this behavior. A linear strain-hardening region is then observed after the knee yielding and corresponds to a linear plastic behavior (Henriksson et al. 2008). The ultimate tensile strength and strain at break become higher as a result of the presence of NFC, which clearly improves the fiber-fiber load transmission in the plastic region. This enhancement can already be observed with the addition of only 3 wt% of NFC. Strength at break in this region has been explained as a consequence, mainly, of fiber slippage (Henriksson et al. 2008; Sehaqui et al. 2011). The reinforcing mechanism of

NFC added to fiber-based biocomposites has been explained as a consequence of several phenomena. Since biocomposites were prepared from aqueous suspensions, the formation of strong hydrogen bonds between fibers during drying was expected. Besides, the large specific surface area of NFC further promotes the formation of hydrogen bonding. Another important feature is the distribution of NFC within the matrix. Several studies have demonstrated that NFC forms a nanometric network embedded between the larger fibers, filling the micropores formed by the larger fibers (Sehaqui et al. 2011). In this way, the material is less porous, and the load-carrying ability of the biocomposite is increased.

Figure 5 illustrates the differences between the neat matrix composed of only unbleached eucalyptus fibers and biocomposites reinforced with 6 wt% of NFC using SEM microphotography. The non-reinforced sample shows a porous, rough surface where fibers are entangled between them but without forming a solid structure. In the picture corresponding to the reinforced sample, we can observe a less porous material because of the filling effect that NFC has on the biocomposite, thus forming a more compact fiber network.

#### Theoretical prediction of mechanical properties of biocomposites

By analyzing the mechanical test results of biocomposites through the modified rule of mixtures (Eqs. 1 and 3), it is possible to determine the coupling factor ( $f_c$ ) and the efficiency factor ( $\eta_e$ ) of biocomposites.

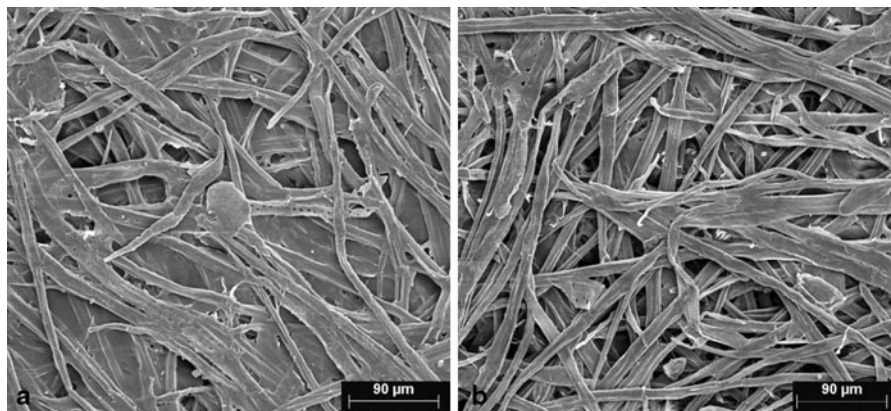


**Fig. 5** SEM microphotographs of biocomposites: **a** sample reinforced with 6 wt% of NFC; **b** neat matrix without any reinforcement

**Table 4** Volume fraction, tensile strength and Young's modulus from biocomposites used in this work and the coupling factor ( $f_c$ ) and efficiency factor ( $\eta_e$ ) calculated from every corresponding sample

NFC (wt%)	V <sup>F</sup>	$\sigma_t^{bc}$ (MPa)	$f_c$	$E_t^{bc}$ (GPa)	$\eta_e$
0	0	19.75 ± 2.07	0	3.85 ± 0.45	0
3	0.011	32.75 ± 3.26	0.175	4.41 ± 0.19	0.345
6	0.022	41.30 ± 2.81	0.145	5.30 ± 0.28	0.434
9	0.035	50.05 ± 6.80	0.128	6.12 ± 0.45	0.427
12	0.045	53.20 ± 5.40	0.110	5.95 ± 0.33	0.314

Table 4 presents the tensile strength and Young's modulus for every set of samples and the values of  $f_c$  and  $\eta_e$  calculated thereof. The volume fraction was obtained from the sample's density (Table 3) and by assuming the density of cellulose to be 1.6 g/cm<sup>3</sup>. The coupling factor was calculated by considering  $\sigma_t^{NFC}$  as 6919 MPa and  $\sigma_t^{m*}$  as 19.75 MPa, corresponding to the experimental tensile strength of the neat matrix. It is important to mention that, according to Manninen et al. (2011), it is possible that the amount of NFC retained decreases as more NFC is added even though cationic starch is used as a retention agent in the slurry. This means that the calculated volume fraction of NFC might be over the real values. As a result, the real coupling factor would be slightly inferior to the calculated one.

The results showed that  $f_c$  decreased as more NFC was added, finding its lowest value in samples with 12 wt% of reinforcement. Since  $f_c$  represents the degree of adhesion between the reinforcement and the matrix, a decrease would indicate deterioration in the interaction between nanofibrils and larger fibers. In the case of  $\eta_e$ , determined by considering  $E_t^{NFC} = 161.05$  GPa and  $a = 3.85$  GPa, it presented an average value close to 0.4, which is typical of composite materials. This behavior in both coupling and efficiency factors can be attributed to poor dispersing conditions during the preparation of the biocomposites, indicating that, as more NFC is added to the slurry, the application of more energy becomes necessary to achieve better dispersion and interaction between the nanofibrils and the larger fibers. In order to observe how the number of revolutions applied during dispersion affects the performance of NFC within the matrix, biocomposites reinforced with 3 wt% of NFC were fabricated by previously dispersing the fiber slurry at different

**Table 5** Evolution of mechanical properties, coupling factor ( $f_c$ ) and efficiency factor ( $\eta_e$ ) in biocomposites reinforced with 3 wt% of NFC in relation to the revolutions applied to the eucalyptus/NFC slurry before drying

Dispersion (revolutions)	$\sigma_t^{bc}$ (MPa)	$f_c$	$E_t^{bc}$ (GPa)	$\eta_e$
90000	26.75	0.12	4.05	0.135
180000	32.75	0.18	4.41	0.340
240000	38.60	0.25	4.82	0.570

revolutions. The results from mechanical tests of such biocomposites as well as the coupling and efficiency factor calculated from every case are shown in Table 5.

In Table 5, it is important to note the significant increase of 18 % in tensile strength of samples dispersed at 240000 revolutions compared to those dispersed at only 90000. The coupling factor also presented important enhancement, and the value of 0.25 for biocomposites dispersed at 240000 revolutions is very close to the maximum of 0.28 reported for plastic composites (Fu and Lauke 1996). The same trend was observed in Young's modulus; the increase in biocomposites dispersed at maximum revolutions was 12 % in comparison to samples dispersed at 90000. The efficiency factor also improved until reaching a value of 0.57, very similar to that described by other authors (Sanadi et al. 1994; Gironés et al. 2007). Furthermore, by using the coupling and efficiency factors corresponding to samples dispersed at 240000 revolutions, it is possible to predict the tensile strength and Young's modulus for all the other biocomposites and compare them to experimental results (Fig. 6). An enhancement and linear evolution of mechanical properties can be observed for either experimental or predicted results.

The predicted results for tensile strength were considerably higher than the experimental ones, and the difference became wider with increasing content of NFC, whereas values for Young's modulus, though superior to experimental ones, were not as pronounced as in tensile strength. Thus, it becomes clear that dispersion is one of the key factors behind the reinforcing effect of NFC in all-cellulose biocomposites, mainly when the NFC content is above 3 wt%. These results also confirm the great reinforcing potential that NFC can provide.

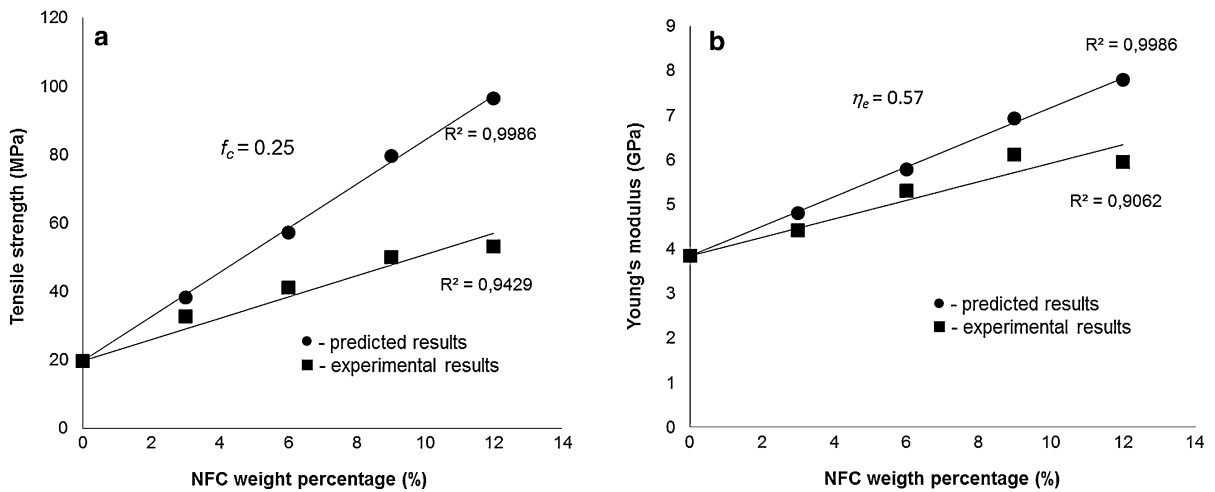


**Fig. 6** Tensile strength (a) and Young’s modulus (b) of biocomposites: comparison in evolution between the predicted values (filled circle) and experimental ones (filled square). The

coupling and efficiency factors used for calculating the predicted results are shown above the tendency line

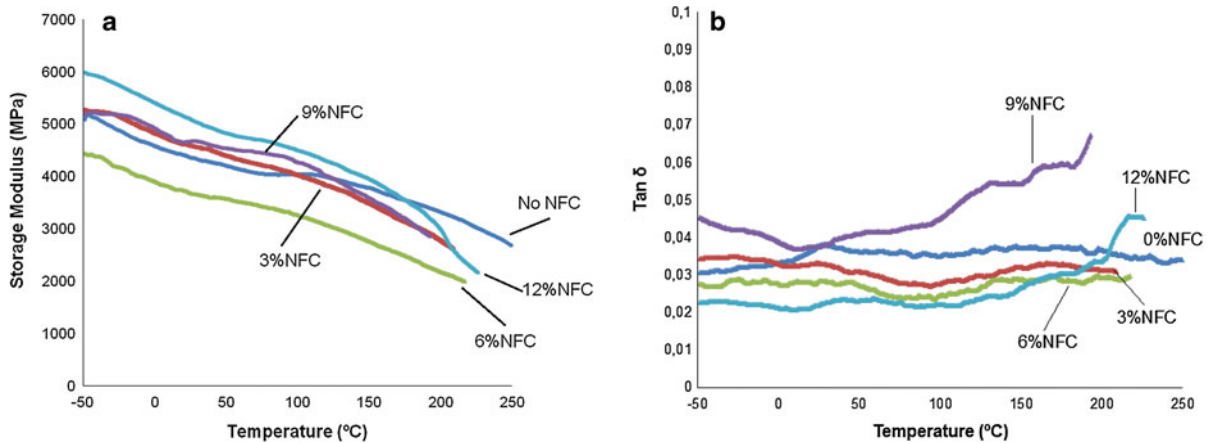


**Fig. 7** Storage modulus (a) and tanδ (b) as a function of temperature for all the composite materials. Percentage of NFC indicates the solid content by weight of NFC

DMTA analysis of biocomposites

To gain further insight into the thermo-mechanical behavior of the biocomposite and the change in stiffness with temperature, the mechanical properties in the linear range were analyzed using DMTA. Results shown in Fig. 7 indicate a maintaining of the storage modulus E’ within the range of 6–3 GPa over the domain of temperature ranging from –50 up to 150 °C, although a small drop in E’ is noted in between as the temperature is going up. This phenomenon might be associated with the damage in the bonding network connecting the NFC to the cellulose fibers.

Actually, as the strength of the NFC network is driven by the hydrogen bonding between the connected area involving the fibers and NFC, an increase in the temperature over several tens of degrees will inevitably cause a drop in the strength of the interaction.

The quite high value of E’ is indicative that the high stiffness of the biocomposite is preserved until the materials start degrading. The moderate drop of E’ by a factor of about 20 % as the temperature goes across 0 °C might be the effect of the adsorbed water on the biocomposite.

However, unlike the data obtained from non-linear analysis (tensile measurement), the modulus does not

show a continual increase with the MFC content. Actually, in the temperature range of 20–25 °C, the value of  $E'$  remained roughly constant around 4.5 GPa for the biocomposite, with NFC content up to 9 %. The only positive shift in the  $E'$  curve is noted for the sample with 12 % NFC. However, these results should be not viewed as a disagreement with the tensile test data. Indeed, as the NFC content increases, accurately sensing the increase in the degree of stiffness of the sample is not so important in DMTA analysis. In fact, the great difficulty to perfectly determine the sample thickness of the biocomposite (due to its surface roughness) along with the great sensitivity of DMTA measurement, specifically for rigid samples, to any fluctuation in the sample dimension might account for the difficulty in noting any notable evolution in the stiffness of the paper biocomposite using the DMTA technique. The  $\tan\delta$  curves are also presented in Fig. 7. No meaningful change is observed up to a temperature of 200 °C, indicating the lack of any molecular relaxation within this temperature range. This is expected, since cellulose, which is the main component of the biocomposite, does not exhibit any thermal transition (glass transition or melting) up to the thermal degradation.

## Conclusions

Biocomposites based on unbleached eucalyptus pulp as the matrix and reinforced with NFC were fabricated. The effect of NFC on the biocomposites' properties was later studied, showing an excellent reinforcing capacity of NFC. Tensile strength and Young's modulus improved linearly, increasing up to 150 and 60 %, respectively, in biocomposites reinforced with 9 wt% of NFC. Specific properties followed similar tendencies, whereas work to fracture also presented significant improvement. Moreover, biocomposites became denser as more reinforcement was added, showing a good correlation with the evolution of tensile strength and Young's modulus. As a consequence of increasing density, the porosity decreased. Calculation of intrinsic mechanical properties of NFC allowed verifying the mechanical behavior of biocomposites for both tensile strength and Young's modulus. The results also permitted calculating the coupling and efficiency factors ( $f_c$  and  $\eta_c$ , respectively), which presented values very similar

to those reported for composites with polymeric matrices. Finally, it was also demonstrated that dispersion of NFC significantly improves the properties in biocomposites as well as both coupling and efficiency factors.

**Acknowledgments** The authors are thankful to the Spanish Ministry of Science and Innovation for the financial support given by the projects CTQ2010-21660-C03-03 and CTM2011-28506-C02-01 to develop this study.

## References

- Besbes I, Rei Vilar M, Boufi S (2011) Nanofibrillated cellulose from alfa, eucalyptus and pine fibers: preparation, characteristics and reinforcing potential. *Carbohydr Polym* 86:1198–1206
- Carrasco F, Mutjé P, Pèlach MA (1998) Control of retention in paper-making by colloid titration and zeta potential techniques. *Wood Sci Technol* 32:145–155
- Chakraborty A, Sahin M, Kortschot M (2006) Reinforcing potential of wood pulp-derived microfibrils in a PVA matrix. *Holzforschung* 60:53–58
- Da Silva D, Montanari S, Vignon M (2003) TEMPO-Mediated Oxidation of Cellulose III. *Biomacromolecules* 4:1417–1425
- Dang Z, Zhang J, Ragauskas AJ (2007) Characterizing TEMPO-mediated oxidation of ECF bleached softwood kraft pulps. *Carbohydr Polym* 70:310–317
- Fu SY, Lauke B (1996) Effects of fiber length and fiber orientation distributions on the tensile strength of short-fiber-reinforced polymers. *Compos Sci Technol* 10:1255–1258
- Gironés J, Méndez JA, Boufi S, Vilaseca F, Mutjé P (2007) Effect of silane coupling agents on the properties of pine fibres/polypropylene composites. *J Appl Polym Sci* 6: 3706–3717
- González I, Vilaseca F, Alcalà M, Pèlach MA, Boufi S, Mutjé P (2013) Effect of the combination of biobeating and NFC on the physico-mechanical properties of paper. *Cellulose* 20:1425–1435
- Henriksson M, Berglund LA, Isaksson P, Lindström T, Nishino T (2008) Cellulose Nanopaper Structures of High Toughness. *Biomacromolecules* 9:1579–1585
- Henriksson M, Fogelström L, Berglund LA, Johansson M, Hult A (2011) Novel nanocomposite concept based on cross-linking of hyperbranched polymers in reactive cellulose nanopaper templates. *Compos Sci Technol* 71:13–17
- Iwamoto S, Kai W, Isogai A, Iwata T (2009) Elastic Modulus of Single Cellulose Microfibrils from Tunicate Measured by Atomic Force Microscopy. *Biomacromolecules* 9:2571–2576
- Kalapurad G, Joseph K, Thomas S (1997) Theoretical modeling of tensile properties of short sisal fibre-reinforced low-density polyethylene composites. *J Mater Sci* 32: 4261–4267
- Klemm D, Kramer F, Moritz S, Lindström T, Ankerfors M, Gray D, Dorris A (2011) Nanocellulose: a new family of nature-based materials. *Angew Chem Int Ed* 50:5438–5466
- López JP, Méndez JA, El Mansouri NE, Mutjé P, Vilaseca F (2011) Mean intrinsic mechanical properties of stone groundwood fibers from softwood. *Bioresources* 6:5037–5049

- Lue J, Wang T, Drzal LT (2008) Preparation and properties of microfibrillated cellulose polyvinyl alcohol composite materials. *Compos A Appl Sci Manuf* 39:738–746
- Manninen M, Kajanto I, Happonen J, Paltakari J (2011) The effect of microfibrillated cellulose addition on drying shrinkage and dimensional stability of wood-free paper. *Nordic Pulp Paper Rese* 26(3):297–305
- Marais A, Wågberg L (2012) The use of polymeric amines to enhance the mechanical properties of lignocellulosic fibrous networks. *Cellulose* 19:1437–1447
- Mark RE (1967) Cell wall mechanics of tracheids. Yale University Press, New Haven
- Molin U, Daniel G (2004) Effects of beating on the fibre structure of kraft pulps as revealed by FE-SEM and TEM: influence of alkaline degradation. *Holzforschung* 58:226–232
- Mutjé P, Pèlach MA, Vilaseca F, García JC, Jiménez L (2005) A comparative study of the effect of refining on organosolv pulp from olive trimmings and kraft pulp from eucalyptus wood. *Bioresour Technol* 96:1125–1129
- Mutjé P, Pèlach MA, García JC, Presta S, Vilaseca F, Jiménez L (2006) Comparison of cationic demand between olive wood organosolv pulp and eucalyptus kraft pulp. *Process Biochem* 41:1602–1607
- Orblin E, Fardim P (2011) Interactions between cationic polyelectrolyte and pulp fines. *Bioresources* 6:2340–2355
- Pèlach MA, Pastor FJ, Puig J, Vilaseca F, Mutjé P (2003) Enzymatic deinking of old newspapers with cellulase. *Process Biochem* 38:1063–1067
- Qua EH, Hornsby PR, Sharma HSS, Lyons G, McCall RD (2009) Preparation and Characterization of Poly(vinyl alcohol) Nanocomposites Made from Cellulose Nanofibers. *J Appl Polym Sci* 113:2238–2247
- Rodríguez M, Rodríguez A, Bayer J, Vilaseca F, Gironés J, Mutjé P (2010) Determination of corn stalk fibers' strength through modeling of the mechanical properties of its composites. *Bioresources* 5:2535–2546
- Rouger J, Mutjé P (1984) Correlation between the cellulose fibers beating and the fixation of a soluble cationic polymer. *Br Polym J* 16:83–86
- Saito T, Kurumae R, Wohler J, Berglund LA, Isogai A (2013) An ultrastrong nanofibrillar biomaterial: the strength of single cellulose nanofibrils revealed via sonication-induced fragmentation. *Biomacromolecules* 14:248–253
- Sanadi AR, Young RA, Clemons C, Rowell RM (1994) Recycled newspaper fibers as reinforcing fillers in thermoplastic: 1. Analysis of tensile and impact properties in polypropylene. *J Reinf Plast Compos* 13:54–67
- Sehaqui H, Allais M, Zhou Q, Berglund L (2011) Wood cellulose biocomposites with fibrous structures at micro- and nanoscale. *Compos Sci Technol* 71:382–387
- Spence KL, Venditti RA, Rojas OJ, Habibi Y, Pawlak JJ (2011) A comparative study of energy consumption and physical properties of microfibrillated cellulose produced by different processing methods. *Cellulose* 18:1097–1111
- Vilaseca F, López A, Llauro X, Pèlach MA, Mutjé P (2004) Hemp strands as reinforcement of polystyrene composites. *Chem Eng Res Design* 82:1425–1431
- Vilaseca F, Valadez-González A, Herrera-Franco PJ, Pèlach MA, López JP, Mutjé P (2010) Biocomposites from abaca strands and polypropylene. Part I: evaluation of the tensile properties. *Bioresour Technol* 1:387–395
- Wainwright SA, Biggs WD, Currey JD, Gosline JM (1982) Mechanical design in organisms. Princeton University Press, Princeton
- Yano H, Nakahara S (2004) Bio-composites produced from plant microfibril bundles with nanometer unit web-like network. *J Mater Sci* 39:1635–1638
- Young RJ, Lovell PA (1981) Introduction to Polymers, 2nd edn. CRC Press, Boca Raton, pp 319–321
- Zimmerman T, Pöhler E, Geiger T (2004) Cellulose fibrils for polymer reinforcement. *Adv Eng Mater* 6:754–761